

When Cognitive Graphs Meet LLMs: BDEI Cognitive Pathways for Panic Emotional Arousal Prediction

1st Mengzhu Liu and Long Qin
College of Systems Engineering

National University of Defense Technology
Changsha, China
{liumengzhu2001, qinlong}@nudt.edu.cn

2nd Chuan Ai* and 3rd Zhengqiu Zhu*
College of Systems Engineering

National University of Defense Technology
Changsha, China
{aichuan, zhuzhengqiu12}@nudt.edu.cn
*Corresponding author.

4th Hongru Liang
College of Computer Science
Sichuan University
Chengdu, China
lianghongru@scu.edu.cn

5th Chen Gao and 6th Yong Li

BNRist
Tsinghua University
Beijing, China

{chgao96, liyong07}@tsinghua.edu.cn

7th Xin Lu

College of Systems Engineering
National University of Defense Technology
Changsha, China

xin.lu.lab@outlook.com

8th Quanjun Yin

College of Systems Engineering
National University of Defense Technology
Changsha, China

yin_quanjun@163.com

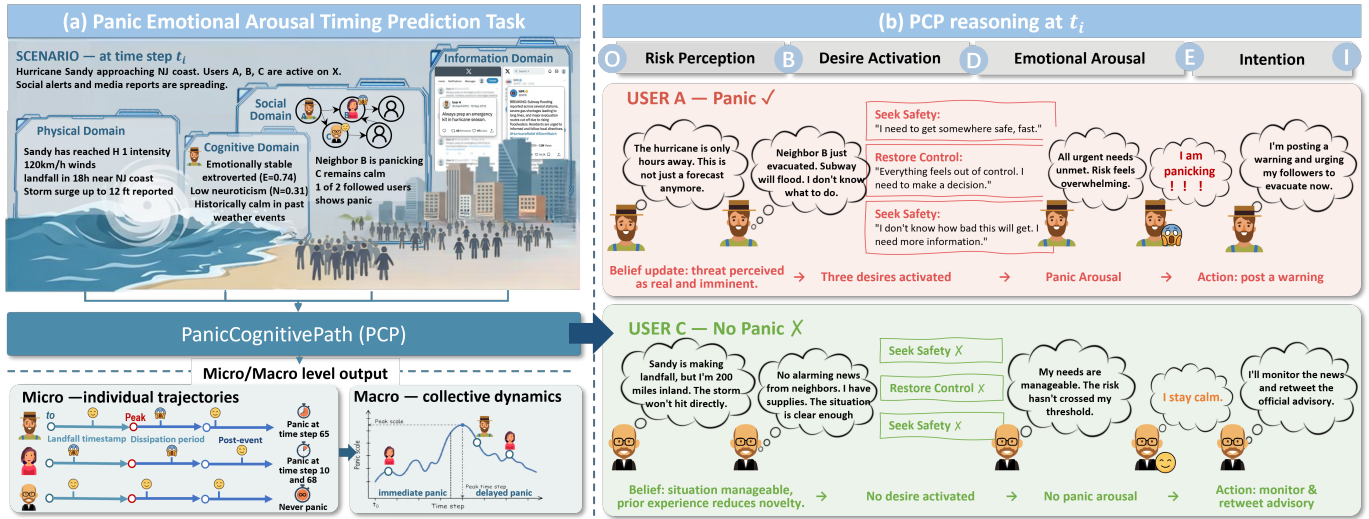


Fig. 1: Multi-domain coupling for panic arousal timing and macro outbreak prediction. (a) Task formulation. At the time step t_i , physical, social, cognitive and information inputs drive PCP reasoning to predict each individual's panic arousal timing and the macro peak panic scale and its time step. (b) PCP reasoning at step t_i . User A activates all three desires and panics; User C perceives lower risk, activates no desire, and stays calm.

Abstract—Predicting individual panic emotional arousal timing before manifestation is essential for proactive emergency intervention. Existing methods incorporate cognitive elements but none explicitly model the emotional arousal process, making them ill-suited for emotional arousal timing prediction. We argue that grounding prediction in appraisal emotion theory is necessary because it explicitly models this process, but three problems must be solved. (1) Appraisal theory posits that emotion arises from simultaneous evaluation across multiple threat dimensions, yet no prior work fuses these inputs into risk perception. (2) Existing cognitive models lack an Emotion node, decoupling threat appraisal from emotional arousal and forcing

emotions to be inferred indirectly from behaviors. (3) Given their generalizable cognitive reasoning, current approaches adopt LLMs as the primary decision-maker, yet overlook the fragility and hallucination-proneness of their outputs. To address these issues, we introduce PanicCognitivePath (PCP), a framework that addresses all three. A Psychological Safety Distance (PSD) model, grounded in psychological distance theory, maps four-domain signals into a unified risk metric as the entry condition for subsequent cognitive reasoning. An explicit Emotion node grounded in appraisal emotion theory is introduced into BDI, forming a Belief-Desire-Emotion-Intention (BDEI) pathway. Agents whose risk metric exceeds the PSD threshold enter

this pathway, coupling threat appraisal directly to emotional arousal. The BDEI pathway governs all state transitions while the LLM is confined to parameter estimation for the Belief-to-Desire transition, confining hallucinations to a single step and preventing error propagation. Experiments on Hurricane Sandy show PCP improves arousal timing accuracy by 10.68%¹ over baselines, reduces peak count error to 7.07%. Implementation is available at <https://github.com/supersonic0919/PanicCognitivePath>.

Index Terms—Panic arousal prediction, Multi-domain coupling, BDEI cognitive pathway, Large language model.

I. INTRODUCTION

Panic emotional arousal (abbreviated as panic arousal thereafter) during emergencies can transform affected populations into secondary hazard sources, as its propagation often exceed the physical damage itself [1]. For instance, after the 2010 Chilean magnitude-8.8 earthquake, panic-driven looting compounded the original disaster [2]. This motivates the task of panic arousal prediction: as illustrated in Figure 1, given only the observable emergency attributes, can we predict each individual’s panic arousal timing and the collective peak scale with its time step before panic manifests? Such prediction enables preemptive intervention.

Existing approaches to panic arousal timing prediction include differential equation models and agent-based simulations, which rely on averaged population assumptions or predefined rules [3]. Further, some integrate the Belief-Desire-Intention (BDI) architecture into agent modeling [4], introducing structured reasoning from beliefs and desires to intentions. More recently, LLM-driven generative agents offer contextual reasoning [5], with improvements via knowledge graphs [6], [7], retrieval-augmented generation [8], and chain-of-thought prompting. However, these approaches neglect to model the emotional arousal process. The transition from risk perception to arousal remains unmodeled, leaving predictions of arousal timing without psychological fidelity.

We argue that grounding panic arousal timing prediction in appraisal emotion theory [9] is necessary because it explicitly models how emotional arousal arises from cognitive appraisal of events. To achieve this, three challenges must be addressed. **(1) Appraisal involves stimuli from multiple domains, yet no prior work fuses physical, social, cognitive, and informational signals into a unified representation.** Consider a hurricane scenario: a resident’s panic depends on how close the storm is (physical), whether neighbors are panicking (social), whether they acutely perceive the risk (cognitive), and what the news reports (informational). Without such fusion, the model captures only partial risk signals, falling short of the comprehensive threat evaluation that appraisal theory requires. **(2) Existing cognitive models infer emotions indirectly from behaviors rather than explicitly modeling their formation process.** Without an explicit Emotion node, the process from risk perception to panic arousal remains implicit and untraceable. For instance, if a traditional model predicts panic for a user at some time step, one cannot verify whether this

follows a valid cognitive process or reflects spurious correlations. Even with a complete cognitive pathway, parameterizing individual-level transitions from threat perception to desire activation requires sensitivity to personal heterogeneity. **(3) Given their generalizable cognitive reasoning, current approaches adopt LLMs as the primary decision-maker, yet overlook the fragility and hallucination-proneness of their outputs.** Once the LLM produces a hallucinated emotional response at one step, this error propagates and amplifies across subsequent simulation steps. Without circumscribing the LLM within a structured pathway, outputs become unreliable [10].

To address these challenges, we propose **PanicCognitivePath (PCP)**, a BDEI (Belief-Desire-Emotion-Intention) cognitive path framework. **(1) To address the risk perception representation challenge**, we construct a psychological safety distance model (PSD) for mapping heterogeneous four-domain signals into a unified risk metric, which determines pathway entry via a safety threshold. **(2) To address the pathway challenge**, we introduce an explicit Emotion node grounded in appraisal emotion theory into BDI, forming a BDEI pathway. This node couples threat appraisal directly to emotional arousal, making the threat-to-arousal transition a traceable cognitive step. **(3) To address the reliability challenge**, we constrain the LLM to parameter inference for only the Belief-to-Desire transition within the BDEI pathway. Rigid rule-based thresholds cannot capture how individual traits and situational contexts jointly shape desire activation, making the LLM’s contextual reasoning necessary. However, placing the LLM at the center of decision-making allows hallucinations to propagate across steps. By confining the LLM to a well-defined subtask within a structured cognitive graph, hallucinations are isolated to a single step and cannot cascade.

Our contributions are summarized as follows:

- **Conceptually**, we ground panic emotional arousal timing prediction in appraisal emotion theory, recognizing that existing methods fail because they lack a model of the emotional arousal process. We identify three sequential barriers to achieving this grounding, reframing the task from behavior prediction to psychologically grounded emotion timing prediction.
- **Methodologically**, we propose PCP, integrating a psychological safety distance model for unified risk perception, a BDEI pathway with an explicit Emotion node, and a constrained LLM role that performs only parameter inference. The structured cognitive graph governs all state transitions, making the panic arousal process traceable and confining LLM hallucinations to a single step.
- **Experimentally**, we curate a Hurricane Sandy dataset with three-class individual panic arousal labels (none/immediate/delayed panic) and evaluate PCP against 12 baselines. PCP improves individual arousal timing accuracy by 10.68 percentage points, reduces peak panic count error to 7.07%. These results demonstrate that explicit modeling of the emotional arousal process enables both accurate individual prediction and faithful collective dynamics.

¹All percentage symbols (%) in this paper denote percentage points (pp.) unless otherwise specified.

II. RELATED WORK

A. Traditional Simulation Models of Emotion Propagation

Social simulation under emergencies relies on dynamic models and ABMs. Epidemic-derived models (e.g., SIS/SIR, SLIRS [11], SI-SEIR [12]) treat emotions as pathogen transmission. Although efficient at the macro level, they reduce arousal to state probabilities and miss individual cognition and multi-domain coupling [13]. ABMs and social force models allow heterogeneity but use rigid rules that cannot model implicit perception-to-arousal pathways [14]. Both share two limitations: 1) reducing arousal to probabilistic transitions while ignoring how individuals cognitively appraise threats; 2) relying on single-dimensional data, which fails to capture how physical hazards, social ties, and information exposure jointly shape panic, leaving the model blind to cross-domain interactions that drive real-world arousal.

B. LLM-Driven Social Simulation

Recent years have seen a growing trend of using LLM-based agents for social simulation in domains such as transportation, economics, and public opinion. Park et al. showed that LLM-driven agents replicate social behaviors via reflection and planning [15], with recent platforms (AgentSociety [16], LAID [17], YuLan-OneSim [18]) further enhancing fidelity through natural language interaction. Researchers have also adopted GraphRAG to ground agent reasoning in structured knowledge [6], [7], [19]. However, applying LLMs to panic simulation remains problematic. Current LLM-driven approaches place the model at the center of reasoning, leading to unstable, prompt-sensitive outputs and accumulated hallucination across simulation steps. Moreover, purely LLM-driven agents lack computable coupling with external multi-domain data, and their opaque reasoning chains cannot produce traceable arousal predictions required for risk assessment [8].

C. Cognitive Architectures and Psychological Foundations for Agent Emotion Modeling

Psychologically, appraisal theories (e.g., OCC [20], [21]) posit that emotions arise from structured event appraisal, providing a foundation for emotion simulation. Yet existing implementations oversimplify elicitation pathways, neglect intuition-based emotions and psychological safety distance, and cannot dynamically integrate multimodal cues for panic arousal timing prediction [22]. Furthermore, the BDI cognitive architecture formalizes rational agent behavior in multi-agent systems [23], [24], but lacks affective states, failing to capture rapid, implicit arousal under acute threat. Emotion propagation theory holds that affective states spread via primitive mimicry and feedback [25] across physical and online channels, precisely the multi-domain coupling that existing computational models fail to operationalize.

III. PROBLEM DEFINITION

A. Definition of Panic Arousal Timing

Panic propagation in crises exhibits salient temporal characteristics that distinguish it from panic emotion recognition.

While recognition tasks identify whether an individual is panicking at a given moment, propagation demands predicting when and how quickly arousal spreads across a population over time. To quantify this dynamic, we define it at the level of micro-individual psychological processing.

At the individual level, panic arousal time refers to the time interval from an individual a_i 's first exposure to information stimulus from emergency event E to the moment when their internal psychological state exceeds the panic threshold θ_{panic} . This process encompasses not only the physical arrival time of information, but also the psychological time required for individuals to process information through cognitive appraisal based on their psychological schemas. Formally, let t_0 denote the initial time of the emergency event, and let $s_i(t)$ denote the panic intensity of individual a_i at time t . The panic arousal time τ_i of individual a_i is then defined as follows:

$$\tau_i = \min\{t \geq t_0 \mid s_i(t) \geq \theta_{\text{panic}}\} \quad (1)$$

If the individual never reaches the panic threshold throughout the simulation cycle, $\tau_i = \infty$.

At the macro level, let $N(t) = |\{a_i \mid s_i(t) \geq \theta_{\text{panic}}\}|$ denote the number of panicking individuals at time t . The collective eruption dynamics are characterized by the peak panic count $N^* = \max_t N(t)$ and the peak time step $t^* = \arg \max_t N(t)$.

B. From Behavior Inference to Emotional Arousal Modeling

Existing approaches implicitly adopt a behavior-bridged inference paradigm that predicts observable behaviors and then inversely infers emotional states, recovering emotion indirectly through a two-step backward chain rather than directly modeling the emotional arousal process. We formally define both paradigms to highlight their fundamental difference.

1) *Behavior-Bridged Inference*: Given the single-domain prior information $D_{\text{phy}}/D_{\text{soc}}/D_{\text{cog}}/D_{\text{info}}$ at time t_0 of emergency E , and the emotional labels $Y = \{y_i\}_{i=1}^n$ ($y_i \in \{0, 1\}$), the task solves for a composite mapping Φ :

$$\Phi : (D, Y \mid E, t_0) \xrightarrow{f_{\text{beh}}} B \xrightarrow{f_{\text{inv}}} \{(\hat{y}_i, \hat{\tau}_i)\}_{i=1}^n \quad (2)$$

where f_{beh} maps the single-domain input D to behavioral traces B , and f_{inv} inversely recovers the panic state $\hat{y}_i \in \{0, 1\}$ and arousal time $\hat{\tau}_i \in \mathbb{R}^+$ (if $\hat{y}_i = 1$; else undefined) from B . This paradigm has two limitations. First, the inverse step has no cognitive guarantee since different emotions may produce similar behaviors. Second, single-domain input cannot capture how heterogeneous factors jointly drive panic arousal.

2) *Direct Arousal Modeling*: Given the multi-domain prior information $D_{\text{phy}}, D_{\text{soc}}, D_{\text{cog}}, D_{\text{info}}$ at time t_0 of emergency E , the task directly models the forward cognitive appraisal process from stimulus perception to emotional arousal. Formally:

$$\Psi : (D_{\text{phy}}, D_{\text{soc}}, D_{\text{cog}}, D_{\text{info}} \mid E, t_0) \xrightarrow{\text{appraise}} \{(\hat{y}_i, \hat{\tau}_i)\}_{i=1}^n \quad (3)$$

where $\hat{y}_i \in \{0, 1\}$ is the predicted panic label and $\hat{\tau}_i \in \mathbb{R}^+$ is the predicted arousal time from t_0 . Unlike Φ , Ψ is a structured cognitive pathway grounded in appraisal emotion theory. Each

prediction is produced by a traceable cognitive appraisal process that proceeds from stimulus perception through belief formation, desire generation, and emotional arousal to behavioral intention, making the emotional arousal mechanism explicit rather than inverted from behavioral outcomes.

The paradigm shift from Φ to Ψ centers on removing the behavioral bridge. In Φ , this bridge forces emotion to be a post-hoc recovered latent variable rather than a state produced through a traceable psychological process. In Ψ , emotion is generated forward as a first-class state via a structured appraisal pathway with multi-domain fusion as input. Panic arousal timing prediction demands a trustworthy account of how arousal occurs, which only a direct forward cognitive model can provide.

IV. PANICOGNITIVEPATH METHOD

A. Overview

To overcome these limitations, we propose **PCP**, a multi-domain coupled cognitive framework that predicts panic arousal timing before overt manifestation. As illustrated in Fig. 2, PCP transcends single-dimensional and pure LLM approaches by coupling physical, social, cognitive, and informational domains, covering four core elements: external stimulus, social amplification, cognitive processing, and information interaction. Specifically:

- **Physical domain** captures emergency spatiotemporal features (intensity, time, location, secondary/disaster derivatives), characterizing objective disaster severity.
- **Social domain** captures network topology (following/follower relations), quantifying social amplification of risk perception.
- **Cognitive domain** captures psychological heterogeneity (Big Five traits, topic preferences, emotional patterns), establishing differentiated response baselines to crises.
- **Information domain** integrates historical posts and event content, characterizing transmission paths and individual processing patterns.

At the core cognitive level, PCP extends the classical BDI framework [23] with appraisal emotion theory to form a BDEI pathway for panic simulation. As illustrated in Fig. 2, the pathway introduces an explicit Emotion node linking Belief/Desire to behavioral Intention. Events and mental states jointly trigger emotion, which drives expression and intentional behavior; these in turn update mental states and create new outcomes, forming a dynamic causal loop. By formalizing appraisal theory, BDEI decomposes implicit emotion arousal into node-traceable paths, addressing the limitation of BDI’s lack of implicit emotion mechanisms. Details are in Section B.

Within the BDEI pathway, the LLM serves only as parameter inference for the Belief-to-Desire transition, while the structured cognitive graph governs all other state transitions. This role inversion suppresses LLM hallucination and instability while overcoming the rigidity of traditional rule-based models, balancing interpretability with scenario adaptability (details in Sections C–E). The framework outputs each agent’s

Algorithm 1 PCP Framework for Panic Elicitation Prediction

Require: Multi-domain inputs: physical events \mathcal{P} , social network \mathcal{S} , cognitive profiles \mathcal{C} , information history \mathcal{I} ; time steps T ; risk threshold θ_{risk}

Ensure: Individual panic states $\{s_i(t)\}$ and first panic time τ_i for each agent i ; macro propagation rate R_{macro}

```

1: Initialize: panic history  $H \leftarrow \emptyset$ ; results list  $\mathcal{R} \leftarrow \emptyset$ 
2: for  $t = 1$  to  $T$  do
3:   Load current event state  $e_t$  from  $\mathcal{P}$ 
4:   for each agent  $i$  in parallel do
5:     Risk Perception:  $v_i \leftarrow \text{PsychSafetyDistance}(i, e_t, H, \mathcal{S})$ 
6:                                      $\triangleright$  Eq. (4)
7:     if  $v_i \leq \theta_{\text{risk}}$  then
8:        $s_i(t) \leftarrow 0$   $\triangleright$  No risk perceived
9:     else
10:      LLM Role-Playing:  $r_i \leftarrow \text{LLM}_{\text{role}}(i, e_t, \mathcal{S}, \mathcal{C}, \mathcal{I})$ 
11:                                      $\triangleright$  18-question assessment
12:      Cognitive Appraisal:  $f_i \leftarrow \text{CalcFactors}(r_i)$ 
13:                                      $\triangleright$  Awareness, Novelty, Uncertainty, Coping
14:      Desire Activation:  $d_i \leftarrow \text{MapDesires}(f_i)$ 
15:                                      $\triangleright$  Three desires: safety, control, certainty
16:      Panic Generation:  $s_i(t) \sim \text{Bernoulli}(P_{\text{panic}})$ 
17:                                      $\triangleright$  Eq. (5)
18:    end if
19:    Update  $H[i] \leftarrow H[i] \cup \{(t, s_i(t))\}$ 
20:    Record  $\tau_i = \min\{t \mid s_i(t) = 1\}$  if first panic
21:  end for
22:  Macro Propagation: compute infection peak  $I_{\text{peak}} =$ 
23:   $\max_i \sum_j s_j(t)$ ;  $t_{\text{peak}} = \arg \max_t I_{\text{peak}}$ 
24: return  $\{(\tau_i, s_i(t))\}_{i,t}, R_{\text{macro}}$ 

```

panic state per time step (binary: panic/calm) and first arousal time step, supporting both micro-individual prediction and macro-propagation analysis. Algorithm 1 presents the single-step pseudocode for all agents.

B. Construction of BDEI Cognitive Path Graph

To transform panic from an implicit psychological process into a computable, traceable structured pathway, this section constructs the BDEI cognitive pathway graph for extreme emotion (Fig. 3). The graph defines five core nodes and their causal transitions in a directed format, fully characterizing the cognitive chain from disaster event perception to panic arousal.

Node Design. The graph has five node types. Event Outcome(O) encodes physical spatiotemporal features (disaster intensity, time, location, secondary events). Belief (B) represents disaster perception (perceived/not perceived) with risk propensity. Desire(D) captures three psychological states: seeking safety, restoring control, and seeking information, each with quantitative multi-domain features. Emotion(E) outputs (panic/calm). Intention(I) covers behavioral tendencies for downstream propagation dynamics. Following appraisal theory, E lies between D and I as the emotional gate turning motivation into action readiness.

Edge Design. The graph defines five causal transitions: **(1) Risk perception (O→B):** Transfers event information to belief via psychological safety distance, determining whether the agent enters subsequent cognitive processing (Section C); **(2) Desire arousal (B→D):** An LLM role-playing agent evaluates

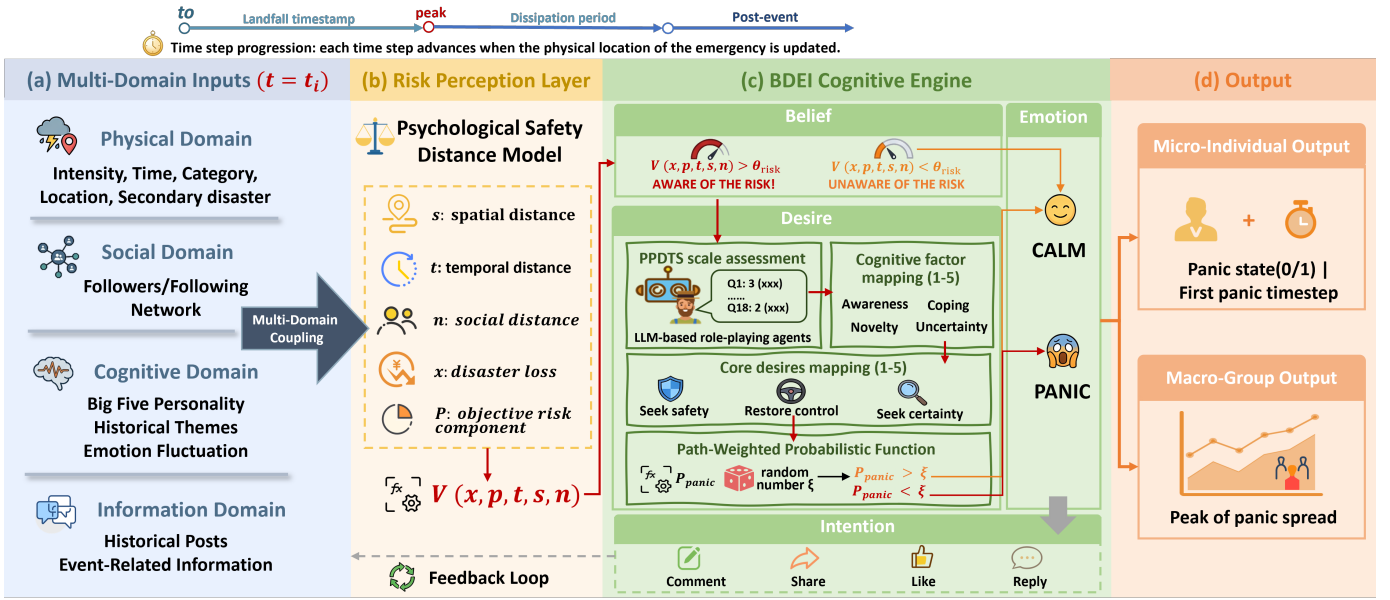


Fig. 2: **Overview of the PCP framework.** Four-domain inputs are coupled via a PSD model into a unified risk metric; agents below the safety threshold enter a BDEI pathway where the cognitive graph governs all transitions and the LLM serves only Belief-to-Desire parameter inference. Outputs include individual panic state and first arousal timestep (micro), and peak panic count with corresponding timestep (macro).

the agent’s psychological state by answering the Psychological Preparedness for Disaster Threats Scale (PPDTS) [26], and the resulting scores are mapped via fixed rules onto four appraisal factors (risk awareness, novelty, uncertainty, and coping efficacy), which are aggregated into the intensity and activation of three core desires (Section D); (3) **Panic arousal (D→E)**: Uses a path-weighted probability function to output binary emotion (0=calm, 1=panic) (Section E); (4) **Behavioral orientation (E→I)**: Captures the influence of emotion on behavioral intention. Targeting propagation speed prediction, we model emotional expression as propagation behavior (updating self state and influencing neighbors) instead of fine-grained actions; (5) **Iterative feedback loop**: Updated belief/emotion states feed into next-step risk perception and social distance, enabling continuous panic simulation.

C. Calculation of Psychological Safety Distance

Psychological Safety Distance (PSD) derives from psychological distance theory [27], [28], which views risk perception as the perceived distance to a risk stimulus. Multi-dimensional distance shapes risk cognition across temporal, spatial, social, and probability dimensions [29], [30]. Greater distance weakens perceived risk through a homogeneous discounting effect [31]. We define PSD as the integrated multi-dimensional psychological distance from an individual to a sudden disaster. PSD is negatively correlated with psychological discounting and positively with subjective risk perception, serving as a core metric for initial disaster risk perception.

We compute PSD based on the Probabilistic Spatiotemporal Trade-off (PTST) model [32], which integrates four psychological distance dimensions, decouples subjective discounting

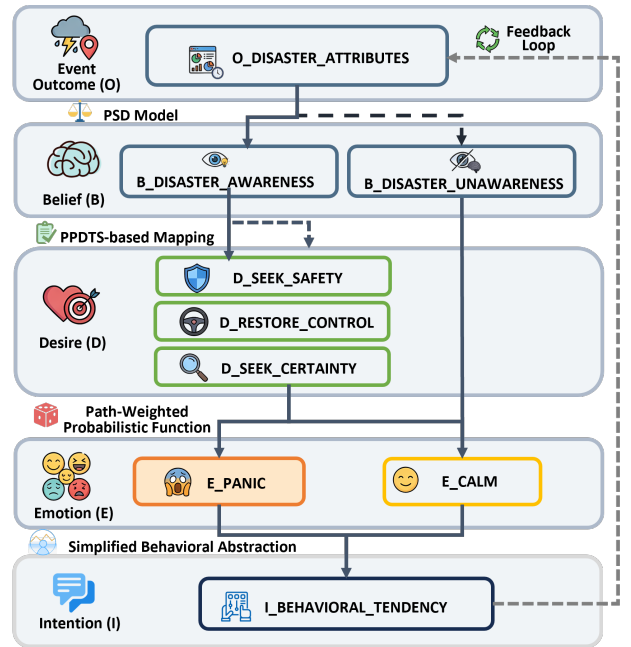


Fig. 3: **BDEI cognitive pathway graph for panic arousal.** The graph formalizes appraisal emotion theory as a causal pathway of five node types (O, B, D, E, I) and sub-nodes, with directed edges annotated by computational models.

from objective risk, and is better suited for quantifying individual risk perception in sudden disasters. Tailored to hurricane-evacuation panic arousal, we adapt its input variables and parameters using PCP multi-domain data, as computed below.

$$V(x, p, t, s, n) = e^{-(a \ln(t+1) + b \ln(s+1) + c \ln(n+1))} \cdot p \cdot x \quad (4)$$

where V denotes the perceived risk level, with a larger value indicating stronger subjective risk perception of the hurricane. The discount function $e^{-(\cdot)}$ aggregates four psychological distance dimensions:

- t : temporal distance, the time-step difference between the current step and disaster occurrence; a : temporal discounting weight;
- s : spatial distance, physical distance to the disaster epicenter; b : spatial discounting weight;
- n : social distance, quantified as the proportion of panic-expressing agents in the agent’s attention list; c : social discounting weight;
- $p \cdot x$: objective risk component, where $p = 1$ for deterministic events and x is the disaster loss, quantified by the hazard intensity level.

We set $a = b = c = 1$, treating all distance dimensions equally. This follows the construal-level theory finding that the four dimensions share a common psychological meaning [33]. They produce similar effects on construal and risk perception, providing no theoretical basis for differential weighting without domain-specific priors.

D. LLM-Assisted Inference for Belief-Desire Transition

For precise B→D transition, we propose an LLM-assisted cognitive mapping method that converts vague disaster perception into quantifiable desire activation states. The method uses PPDTs as a psychometric instrument. An LLM role-playing agent completes the scale based on multi-domain user characteristics and real-time context. Pre-defined rules then map responses to four cognitive factors, which are aggregated into three core desires with activation intensities.

In implementation, an LLM agent builds a personalized profile from cognitive and information domains, integrates real-time physical disaster state and social panic ratio, and follows a 1–4 scale to complete the 18 PPDTs items. Responses reflect the user’s true cognitive state under given constraints. Predefined mapping rules and linear transformation convert raw scores to a 1–5 range, yielding four cognitive factor scores: risk awareness, risk novelty, risk uncertainty, and coping efficacy. These factors represent cognitive depth, experience relevance, situational ambiguity, and self-efficacy, jointly forming the core cognitive appraisal basis for emotion arousal [34]. Based on disaster psychology, these factors are weighted to compute activation intensities for three core desires: seek safety (all four factors), restore control (risk and awareness control-loss), and seek certainty (uncertainty and novelty). A desire activates when its intensity exceeds a threshold. This mechanism, grounded in cognitive appraisal theory and need for cognitive closure [35], translates discrete appraisal dimensions into motivationally significant desire states.

This design converts implicit disaster appraisals into a quantifiable desire set via the B→D transition, providing explicit psychological inputs for subsequent panic arousal. The LLM

serves solely as a reasoning engine for personalized PPDTs responses, avoiding the black-box instability of direct end-to-end prediction while retaining personalization and interpretability.

E. Calculation of panic arousal timing

After computing desire activation and intensity, we propose a D→E state transition mechanism based on desire satisfaction evaluation, transforming multi-desire activation states into binary panic output, achieving computable triggering from intrinsic motivation to panic emotion. The core of this process quantifies the activated desire set and its intensity as a probabilistic judgment of panic occurrence at each time step.

Specifically, panic arousal probability is computed as a path-weighted product along the D→E edge of the BDEI graph, aggregating three activation conditions: (1) the proportion of activated desires N_d to all 3 desire types, reflecting motivation breadth; (2) the average activated desire intensity normalized by the PPDTs score range (1–5), representing urgency of psychological demands; and (3) the normalized PSD influence factor, capturing the amplification effect of objective risk on emotion arousal. Thus, P_{panic} is defined as:

$$P_{panic} = \frac{N_d}{3} \cdot \frac{\bar{I}_d}{5} \cdot \min\left(1, \frac{V}{\theta_{risk}}\right) \quad (5)$$

where \bar{I}_d is the average activated desire intensity, obtained by weighted averaging of individual desire intensities, V is the current PSD, and θ_{risk} is the risk perception threshold.

After obtaining P_{panic} , binary emotion is sampled via $r \sim U(0, 1)$: panic is triggered ($E_{panic} = 1$) if $r < P_{panic}$, otherwise calm ($E_{panic} = 0$). Particularly, when $N_d = 0$ (no desires activated), P_{panic} is directly set to 0, maintaining a calm state (formalized in Eq. 6). This transforms the desire–reality gap into a probabilistic emotion trigger rather than a rigid rule. The stochastic element accounts for uncertainties not captured by the cognitive model, since no model can exhaustively represent all factors influencing individual emotion.

$$E = \begin{cases} 1, & \text{if } r < P_{panic} \text{ and } N_d > 0, \\ 0, & \text{otherwise} \end{cases} \quad (6)$$

In summary, PCP couples multi-domain inputs via a PSD model and decomposes implicit emotion arousal into traceable state transitions along the BDEI pathway. The cognitive graph governs all transitions, while the LLM serves only for Belief-to-Desire parameter inference. This design transforms multi-domain data into dynamic inference from external stimuli to internal emotion, enabling precise panic arousal timing prediction and providing a robust foundation for proactive extreme emotion prevention in emergency social simulations.

V. EXPERIMENTS

A. Experimental Setup

1) *Dataset Construction*: Our experiments use Hurricane Sandy (2012) as the event context, integrating multi-source heterogeneous data to construct a four-domain coupled dataset. We adopt the COPE dataset [36], a fine-grained panic emotion

TABLE I: Dataset Statistics Overview

Statistical Dimension	Value
Number of users	9,065
Total tweets	1,384,989
Pre-disaster tweets	242,363
Post-disaster tweets	1,142,626
Physical domain records	115
Panic users (Immediate)	2,164 (23.87%)
Panic users (Delayed)	1,076 (11.87%)
Non-panic users	5,825 (64.26%)

benchmark constructed through a human-LLM collaborative annotation pipeline. The underlying social media data is derived from a public hurricane dataset [37], covering the following four dimensions:

- **Physical domain:** Hurricane spatiotemporal features and secondary events, from zoom.earth, social platforms, and official media, including 115 records of grade, wind speed, pressure, coordinates, and events descriptions.
- **Social domain:** User follow relationships reconstructed from the Sandy dataset. The social network contains tens of millions of connections, quantifying social distance effects on risk perception.
- **Cognitive domain:** User profiles from the COPE dataset, covering Big Five personality traits, historical emotion trends, tone features, topics of interest, event attitudes, posting frequency, historical posts, and panic emotion labels (binary,0/1). The processed cognitive dataset contains 9,065 users with complete profiles.
- **Information domain:** Disaster-related posts with text, timestamps, user IDs, emotion annotations, geolocation.

The COPE dataset provides binary panic/non-panic labels, lacking differentiation of panic arousal. We refine these labels using the hurricane landfall time (October 30, 2012) as a temporal anchor, subdividing panic into immediate, delayed, and non-panic. Table I presents statistics of our dataset.

2) *Baseline Models:* We compare PCP with four categories of baselines. All use the same 9,065-user dataset, 115 time steps, and evaluation protocol.

- **Traditional dynamics models**

SLIRS [11]: Epidemic contagion analogy with Susceptible-Latent-Infected-Recovered states. We use original parameters ($\mu=0.01$, $\eta=0.05$, $\rho=2$, $\omega=0.9$) with 2% seed users.

BASS [38]: Product diffusion driven by imitation and external innovation coefficients (p , q) calibrated via grid search to match the real peak time.

Voter [39]: An opinion dynamics model where panic is an opinion state updated by stochastic neighbor interaction, with $q=8$, $p=0.03$, $\varepsilon=0.05$.

- **Agent-Based Simulation Models**

ABM-HybridSpaces [40]: Mesa-based agents with demographics, locations, and three-layer networks. 3% seed users with rule-based hurricane intensity response.

Crowd [41]: An BM framework for social network topology, mapping agent attributes to node parameters for lightweight modeling and sharing the same 9,065-node graph with PCP.

SOAR [42]: Cognitive architecture with working memory, rules, and chunking learning. Train on first 70% time steps, test on last 30%. Rule libraries learned from training.

- **End-to-End Prediction Models**

E-USIM [43]: Uses RNN and GRU with historical and current neighbor/personal emotion influence to predict next emotion state. 80/20 random user split with time-series cross-validation.

GODEN [44]: User-cascade bipartite graph via GNN, Neural ODE, and Transformer for next-influencer prediction. Same social graph and user features as PCP.

- **Reasoning-Enhanced Models**

ECR-Chain [45]: LLM causal reasoning guided by cognitive appraisal theory. Uses Qwen 2.5-72B with temperature=0; input features restricted to tweet text and sentiment.

LAIDSim [17]: LLM-enhanced independent cascade diffusion with LLM-generated profiles, BERT-encoded influence, and agent-profile-based semantic mutation. Default parameters ($\alpha=0.5$, $k=2$ seed nodes) from the original paper.

Simple Prompt: Uses template prompts for direct LLM emotion classification, without Chain-of-Thought reasoning.

CPM-RL [46]: Reinforcement learning with cognitive appraisal theory for emotion prediction. Q-learning agents with big-five-mapped hyperparameters and SVM classifier (linear kernel, $C=0.014$); trained on theoretical MDP distributions.

3) *Evaluation Metrics:* To comprehensively evaluate the PCP framework on panic arousal prediction, we construct an evaluation scheme from two dimensions: macro-level propagation trends and micro-level user classification.

- **Macro-level**

Macro-level metrics measure the model’s ability to capture overall panic propagation dynamics, including peak scale and temporal position of the panic curve.

Peak Count: The maximum number of panicking agents during the simulation, reflecting propagation intensity. Smaller deviation from ground truth indicates better performance.

Peak Time Step: The time step at which the panic curve reaches its peak, capturing temporal characteristics and propagation speed. Closer to ground truth is better.

Peak Count Error: Measures prediction accuracy on peak panic scale, expressed as relative error (%); lower is better, where $I(t)$ denotes the number of panicking agents at time t .

$$\frac{|\max(I_{\text{sim}}(t)) - \max(I_{\text{real}}(t))|}{\max(I_{\text{real}}(t))} \times 100\% \quad (7)$$

Peak Time Error: Measures prediction deviation on peak panic timing, capturing the framework’s ability to capture emotion arousal dynamics. Lower is better.

$$|\operatorname{argmax}(I_{\text{sim}}(t)) - \operatorname{argmax}(I_{\text{real}}(t))| \quad (8)$$

- **Micro-level**

Micro-level metrics evaluate the model’s ability to classify individual panic types.

Accuracy: Overall correct prediction rate across three panic types.

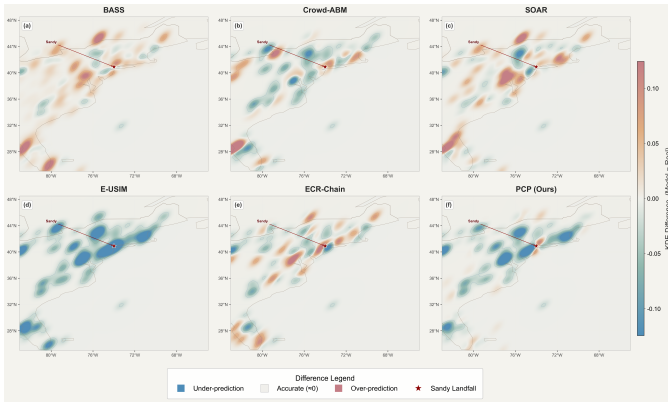


Fig. 4: **Spatial prediction error of peak panic arousal at Step 61 during Hurricane Sandy.** Each panel shows kernel density estimation (KDE) difference (simulated vs. real panic density). Blue: under-prediction; Red: over-prediction; White: accurate match. All KDE heatmaps normalized to $[0,1]$.

Macro F1: Equal-weighted average of per-class F1 scores, mitigating class-imbalance bias and emphasizing minority class (delayed panic) recognition.

Per-class Precision: Proportion of correctly classified samples among those predicted as a given class.

Recall: Proportion of correctly classified samples among all ground-truth samples of a given class.

4) *Implementation Details:* All experiments were conducted on a cloud computing environment equipped with two NVIDIA RTX4090 GPUs. LLM inference employed the Qwen2.5-72B-Instruct model, deployed via a GPU cloud function platform that provides an OpenAI-compatible API. During inference, temperature was set to 0.3 and max_tokens to 1500. The psychological safety distance perception threshold θ_{risk} was set to 0.08, derived by substituting the profile of an average user at the boundary of risk awareness (3-day landfall window, 900 km from storm center, 60% of followed users panicked, Category 1 hurricane) into the PSD formula (4). The desire arousal threshold for the four PPDTs cognitive evaluation factors was set to 3.5 on the 1-5 scale, above the neutral midpoint (3.0), ensuring that only clearly elevated appraisal states trigger desire activation rather than ambiguous or marginal ones.

B. Comparison with SOTA Baselines

We evaluate PCP on Hurricane Sandy against baselines. PCP reduces peak count error to 7.07% and peak time deviation to 2 steps (Table II). Traditional dynamical models assign identical transition rules to all individuals, so a person who panics late from a distant trigger is treated the same as one who panics immediately, yielding peak errors of 65-86%. Agent-based simulations allow individual differences but depend on handcrafted rules, and even SOAR’s best 41.20% cannot capture emergent social media behaviors that violate these rules. Reasoning-enhanced methods let LLMs generate steps without structural constraints, producing exaggerated

outputs with peak errors of 379-950%. Figure 4 confirms this spatially. PCP’s KDE difference at Step 61 is near-zero across most regions, while BASS and ECR-Chain over-predict along the East Coast and E-USIM under-predicts. This fidelity arises from PSD’s four-domain fusion, which lets each agent evaluate psychological safety distance so that a critical mass crossing the threshold naturally produces the observed peak.

PCP achieves 75.66% accuracy and Macro F1 0.5441, leading all baselines by 10.68pp (Table III). Per-class F1 is 0.8730 (non-panic), 0.6401 (immediate), and 0.1194 (delayed). Traditional models assume irreversible or consensus-driven transitions, predicting nearly all users as non-panic (e.g., SLIRS recall 0.02) or as panicked (e.g., BASS recall 0.90). Agent-based simulations similarly default to extremes (e.g., SOAR recall 0.97 versus ABM-HybridSpaces recall 0.05) without cognitive appraisal to differentiate individual threat evaluation. End-to-end models learn from past observations, so delayed panic triggered by future secondary events appears as non-panic, yielding recall below 1.5% for E-USIM and GODEN. Among reasoning-enhanced methods, ECR-Chain over-assigns delayed labels with precision 0.1789 versus recall 0.4786. PCP avoids these extremes by explicitly modeling the appraisal-to-arousal transition, achieving balanced recall (0.87 for Non-Panic, 0.79 for Immediate Panic).

As difficulty increases from non-panic to immediate to delayed panic, PCP’s F1 drops from 0.8730 to 0.6401 to 0.1194, and most baselines show near-zero delayed recall (Table III). This is not method-specific. All baselines lack secondary event modeling that re-triggers panic after the initial hazard subsides. Traditional models use fixed equations with no mechanism for external triggers. End-to-end models learn from past observations, but secondary events lie in the future. SOAR’s rule base covers only the first 70% of time steps. CPM-RL evaluates appraisal independently per step without retaining prior evaluations, so intensity cannot accumulate. Panic arousal requires hazard context, cognitive reappraisal, secondary events, and peer influence. No baseline integrates all four, and PCP itself lacks secondary event modeling, explaining its low delayed panic F1 despite leading otherwise.

C. Ablation Studies

To verify the contribution of each core component in the PCP framework, we design a three-level ablation study: (1) w/o BDEI Path, removes the cognitive pathway structure and uses direct end-to-end panic prediction via LLM with user profiles and disaster context; (2) w/o PSD, removes the PSD model and replaces it with a physical distance threshold for risk perception; (3) w/o LLM, removes LLM-assisted reasoning and replaces PPDTs factor scoring with rule-based mapping from raw Big Five trait scores and contextual features. Results are shown in Tables IV and V.

Results at the macro level show the full model achieves a peak error of 7.07% and a timing deviation of 2 step. Removing either the BDEI pathway (peak error 379.25%) or the LLM (303.76%) causes the simulated panic count to explode by 4-5 \times , indicating that both structured cognitive

TABLE II: Comparison of macro-level propagation dynamics across all baseline models

Category	Model	Peak Count	Peak Time Step	Peak Error (↓)	Time Error (↓)
Traditional Dynamical	SLIRS	186	1	72.03%	60
	BASS	231	45	65.26%	16
	Voter	90	0	86.47%	61
Agent-Based Simulation	ABM-HybridSpaces	271	0	59.25%	61
	Crowd	308	59	53.59%	<u>2</u>
	SOAR	939	58	41.20%	3
End-to-End Prediction	E-USIM	180	68	72.93%	7
	GODEN	19	0	97.14%	61
Reasoning-Enhanced	ECR-Chain	790	61	18.80%	0
	LAIDSim	6985	6	950.38%	55
	Simple Prompt	3187	57	379.25%	4
	CPM-RL	524	0	21.20%	61
PCP (Ours)		712	63	7.07%	<u>2</u>

^aThe ground-truth panic peak occurs at time step 61 with 665 users.

^bBold indicates the best performance in each column. Underlined indicates the second-best performance.

TABLE III: Comparison of micro-level panic classification performance across all baseline models

Category	Model	Overall		Non-Panic			Immediate Panic			Delayed Panic		
		Acc.(↑)	Macro F1(↑)	Pre.(↑)	Rec.(↑)	F1(↑)	Pre.(↑)	Rec.(↑)	F1(↑)	Pre.(↑)	Rec.(↑)	F1(↑)
Traditional Dynamical Models	SLIRS	0.6313	0.2709	0.6418	0.9746	0.7740	0.2091	0.0213	0.0396	-	-	-
	BASS	0.2276	0.1618	0.8889	0.0014	0.0027	0.2381	<u>0.9025</u>	0.3797	0.1194	<u>0.0948</u>	0.1057
	Voter	0.6057	0.2924	0.6435	0.9112	0.7544	0.2240	0.0846	0.1228	-	-	-
Agent-Based Simulation Models	ABM-HybridSpaces	0.6449	0.2907	0.6667	0.9488	0.7831	0.2592	0.0518	0.0864	0.0667	0.0014	0.0027
	Crowd	0.5732	0.3196	0.6439	0.8220	0.7221	0.2552	0.1821	0.2125	0.1647	0.0130	0.0241
	SOAR	0.2424	0.1473	0.7248	0.0136	0.0266	0.2420	0.9700	0.3874	0.0671	0.0177	0.0280
End-to-End Prediction Models	E-USIM	0.6498	0.3483	0.6798	0.9373	0.7880	0.3833	0.1635	0.2292	<u>0.5000</u>	0.0142	0.0276
	GODEN	0.6434	0.2643	0.6435	0.9993	0.7829	0.5789	0.0051	0.0101	-	-	-
Reasoning-Enhanced Models	ECR-Chain	0.5045	0.4419	0.8432	0.5298	0.6507	0.3848	0.4492	0.4145	0.1789	0.4786	0.2604
	LAIDSim	0.3758	0.2665	0.7644	0.2730	0.4023	0.2601	0.8396	0.3972	-	-	-
	Simple Prompt	0.4802	0.3403	0.7642	0.4702	0.5822	0.2976	0.7421	0.4248	0.0952	0.0074	0.0138
	CPM-RL	0.6142	0.2796	0.6396	0.9379	0.7605	0.2004	0.0485	0.0781	-	-	-
PCP (Ours)		0.7566	0.5441	<u>0.8723</u>	0.8736	0.8730	<u>0.5398</u>	0.7860	0.6401	0.8625	0.0641	0.1194

^aBold indicates the best performance in each column. Underlined indicates the second-best performance.

^bA dash (-) indicates that the model assigned no instances to the delayed panic class, resulting in undefined precision, recall, and F1.

TABLE IV: Ablation study results: macro-level metrics

Model	Peak Panic Count	Peak Time Step	Peak Error (↓)	Time Error (↓)	Time Cost
w/o BDEI Path	3187	57	379.25%	4	115h56min
w/o PSD	184	63	72.33%	2	18h30min
w/o LLM	2685	56	303.76%	5	1h30min
Full	712	63	7.07%	2	14h27min

TABLE V: Ablation study results: micro-level metrics

Model	Overall		Non-Panic			Immediate Panic			Delayed Panic		
	Acc. (↑)	F1 (↑)	Pre. (↑)	Rec. (↑)	F1 (↑)	Pre. (↑)	Rec. (↑)	F1 (↑)	Pre. (↑)	Rec. (↑)	F1 (↑)
w/o BDEI	0.4802	0.3403	0.7642	0.4702	0.5822	0.2976	0.7421	0.4248	0.0952	0.0074	0.0138
w/o PSD	0.6138	0.3611	0.6693	0.8539	0.7504	0.3715	0.2666	0.3105	0.1625	0.0121	0.0225
w/o LLM	0.2293	0.1816	0.7167	0.0074	0.0146	0.2579	0.8489	0.3956	0.1057	0.1849	0.1345
Full	0.7566	0.5441	0.8723	0.8736	0.8730	0.5398	0.7860	0.6401	0.8625	0.0641	0.1194

reasoning and LLM-augmented inference are necessary to prevent uncontrolled panic propagation. By contrast, removing PSD yields a milder degradation (72.33%), as physical distance alone provides a rough but insufficient spatial signal for risk differentiation. In terms of computational efficiency, PCP reduces inference time to 14h 27min ($\approx 8\times$ faster than the pure LLM variant), as PSD filters out low-risk users before they enter the BDEI pathway, reducing unnecessary LLM invocations while preserving multi-domain risk perception.

At the micro level, the full model achieves the best overall accuracy (0.7566) and Macro F1 (0.5441). Each ablation exposes a distinct failure mode: w/o LLM over-predicts immediate panic (recall: 0.8489, precision: 0.2579) due to

rigid rule-based thresholds; w/o PSD captures non-panic well (recall: 0.8539) but misses immediate panic (recall: 0.2666), confirming physical distance alone lacks cognitive granularity; w/o BDEI degrades uniformly (Acc: 0.4802) as direct LLM prediction loses the discriminative reasoning chain. Delayed panic remains a shared bottleneck ($F1 < 0.14$ across all variants). The full model achieves the highest precision (0.8625) with a low recall (0.0641), reflecting conservative yet reliable judgments, whereas w/o LLM trades precision for recall. This precision-recall tension is inherent to the structural information bottleneck – an important direction for future improvement.

Collectively, the ablation results validate the PCP design: BDEI ensures theoretical completeness, multi-domain PSD

TABLE VI: CV of Qwen2.5-72B across temperatures

Temp.	Awareness	Novelty	Uncertainty	Coping	Mean
0.0	0.0779	0.0154	0.0387	0.0707	0.0507
0.3	0.1208	0.0385	0.0578	0.0867	0.0759
0.6	0.1249	0.0613	0.0693	0.0895	0.0862
0.9	0.1441	0.0834	0.0816	0.0982	0.1018

^aBold row indicates the configuration used in the main experiment.

TABLE VII: Cross-model CV comparison at $T = 0.3$

Model	Awareness	Novelty	Uncertainty	Coping	Mean
Qwen2.5-72B	0.1208	0.0385	0.0578	0.0867	0.0759
GLM-5.1	0.1145	0.0764	0.0666	0.1060	0.0909
DeepSeek-V3.2	0.0952	0.1261	0.0702	0.1115	0.1007
Qwen3-8B	0.1262	0.1267	0.1045	0.1009	0.1146

^aBold row indicates the model selected for the main experiment.

captures dynamic risk perception, and LLM enables sensitivity to individual heterogeneity. Their synergy drives the full model’s overall superiority over all ablations, with the lowest false positive rate on delayed panic recognition.

D. Robustness Analysis

Since the BDEI scoring module relies on stochastic LLM inference, PPPTS dimension scores must remain consistent across repeated calls under identical inputs. We quantify robustness via the within-group coefficient of variation ($CV = \sigma/\mu$) over $M = 30$ independent runs per (model, temperature, user) triplet, averaged across 10 users. Lower CV indicates higher scoring stability. As no universal CV threshold exists for LLM-based scoring, robustness is evaluated through internal comparison against both the deterministic baseline ($T = 0.0$) and alternative models.

Temperature sensitivity. Figure 5(a) and Table VI report per-dimension and mean CV of Qwen2.5-72B-Instruct across four temperatures. At $T = 0.0$, the model is deterministic (mean CV = 0.051), but deterministic decoding produces rigid, unnuanced responses that fail to capture the cognitive variability inherent in individual-level appraisal. The critical observation is that the CV increment from $T = 0.3$ to $T = 0.6$ is merely $\Delta = 0.010$, indicating $T = 0.3$ lies at the onset of a stability plateau. This confirms $T = 0.3$ offers a favorable trade-off: sufficient sampling diversity while maintaining reproducible scoring.

Model sensitivity. Figure 5(b) and Table VII compare CV at $T = 0.3$. Qwen2.5-72B-Instruct achieves the lowest mean CV (0.076), outperforming GLM-5.1 (0.091), DeepSeek-V3.2 (0.101), and Qwen3-8B (0.115). The advantage is most pronounced in the novelty dimension (CV = 0.039 vs. second-best 0.076). Conversely, Qwen3-8B exhibits the highest CV in three of four dimensions, suggesting insufficient consistency. These results jointly justify selecting Qwen2.5-72B-Instruct at $T = 0.3$ as the primary configuration.

E. Case Study

To validate PCP’s interpretability, we analyze two counterfactual cases as illustrated in Fig. 6. Case 1: a user with high neuroticism ($E = 0.53, N = 0.58$) far from Hurricane Sandy’s

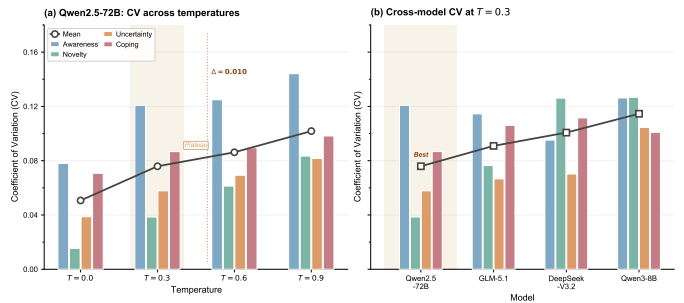


Fig. 5: Robustness analysis of LLM scoring consistency. (a) Per-dimension and mean CV of Qwen2.5-72B-Instruct across temperatures. Shaded: main config $T = 0.3$; $\Delta = 0.010$ at $T = 0.6$ proves stable performance. (b) At $T = 0.3$, Qwen2.5-72B has the lowest and most uniform CV across dimensions.

center. Despite susceptibility to anxiety, large physical distance reduces perceived threat, keeping psychological safety distance well below the panic threshold. The user remains calm, showing how spatial shielding decouples cognitive appraisal from dispositional vulnerability. Case 2: a user with low neuroticism ($E = 0.47, N = 0.52$) in the direct impact zone. Although the stable baseline implies resilience, the convergence of hazard proximity and information escalation compressed the safety distance above threshold, overriding dispositional regulation. Both cases show that multi-domain features interact through cognitive pathways to produce the final emotional state.

F. Discussion

The experiments yield a consistent answer. PCP faithfully reproduces macro-level collective panic emergence while achieving limited yet reliable individual recognition. This dual advantage stems from three synergistic design choices. (1) Multi-domain PSD fusion replaces the single-dimension inputs of prior work. It couples heterogeneous data streams across physical, social, cognitive, and informational domains into a unified safety distance metric. As a result, each agent evaluates threat from multiple perspectives, and the collective peak emerges naturally rather than being distorted by single-factor rules. (2) Explicit BDEI reasoning decomposes the implicit panic formation process into discrete traceable steps. These steps span from risk perception through emotion triggering to intention generation. This makes the cognitive pathway transparent and explainable, rather than a black-box mapping from inputs to labels. (3) Structured LLM constraint confines the model to parameter inference for only the Belief-to-Desire transition. This inverts the conventional role and suppresses hallucination accumulation, while still retaining sensitivity to individual heterogeneity. These three choices are not independent. PSD provides the multi-domain input that BDEI requires, BDEI supplies the pathway structure that constrains the LLM, and the LLM injects the individual variability that rigid cognitive rules alone cannot capture. Their synergy drives the full model’s advantage over all baselines.

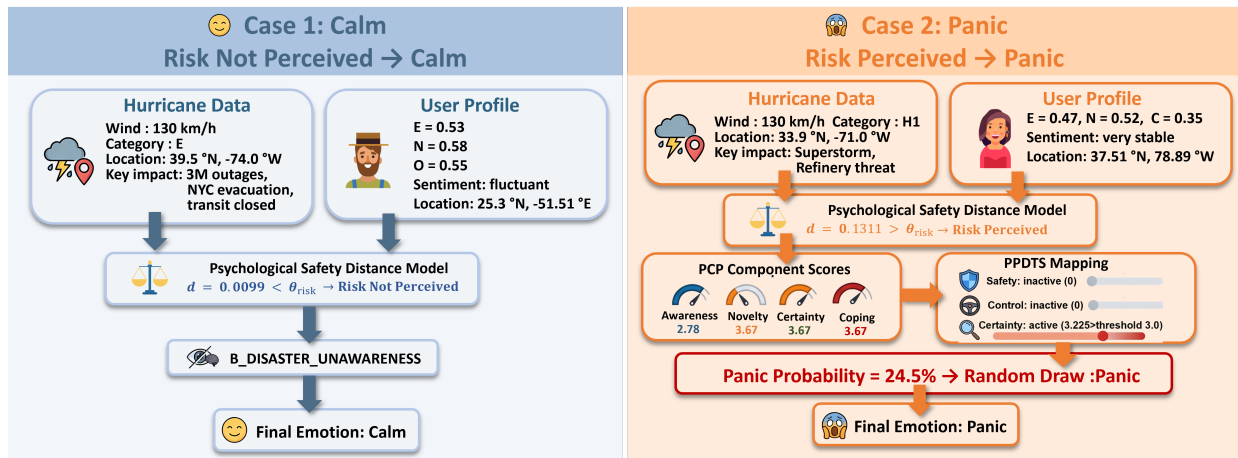


Fig. 6: PCP framework predicts counterfactual panic in a low-neuroticism user (Case 2) by accounting for situational uncertainty and novelty, versus a risk unaware user (Case 1).

The same experimental design also defines the scope of the conclusions. The main limitations are as follows. First, PCP focuses on primary events without fully modeling secondary event interactions on panic arousal, which explains the consistently low delayed panic recall across all models. Second, PCP has been validated only on Hurricane Sandy. Despite domain-general theoretical grounding, its reliance on these theories and PPDTs leaves cross-cultural and cross-disaster generalization unevaluated. Third, PSD discount weights and desire arousal thresholds are determined via domain knowledge and hyperparameter tuning, lacking adaptive optimization that may affect generalization under data shift. Finally, the Emotion-to-Intention transition uses a simplified model, abstracting emotional expression as state updates and propagation without modeling specific behaviors.

These limitations point to four future directions. (1) Incorporating secondary event generation and coupling mechanisms to enable full-trajectory simulation of collective panic arousal, improving both macro-level emergent dynamics reconstruction and delayed panic recognition. (2) Extending PCP to diverse emergency types such as earthquakes and public health events, and exploring adaptation to other extreme emotions. (3) Optimizing the LLM-graph collaborative reasoning architecture with lightweight fine-tuning and dynamic threshold adaptation to improve efficiency while preserving interpretability. (4) Integrating social network behavioral logs to model the emotion-intention-behavior chain in BDEI pathways, achieving full-chain simulation from psychological states to social actions.

VI. CONCLUSION

We ground panic arousal timing prediction in appraisal emotion theory and propose PanicCognitivePath (PCP) as a unified framework. PCP couples heterogeneous data across physical, social, cognitive, and informational domains via a psychological safety distance model. It extends BDI with an explicit Emotion node through a BDEI cognitive pathway. It confines the LLM to parameter inference for only the Belief-

to-Desire transition to suppress hallucination accumulation. Experiments on Hurricane Sandy show that PCP improves arousal timing accuracy by 10.68 percentage points, reduces peak count error to 7.07%, consistently outperforming all baselines. Beyond these empirical gains, the broader implication is that panic arousal prediction can be treated as structured cognitive pathway reasoning rather than only as behavioral pattern fitting or unconstrained LLM generation. More generally, the proposed framework suggests a design principle for psychologically grounded prediction under multi-domain inputs. Fuse heterogeneous data into unified perception metrics. Decompose the target process into traceable cognitive steps. Constrain the LLM to well-defined subtasks within an explicit pathway rather than placing it at the center of decision-making. This perspective connects psychological theory with computational modeling and may be useful for other social simulation problems in which the target process has theoretical structure, multi-domain inputs must be integrated, and generative models need structural guardrails to remain reliable.

VII. ACKNOWLEDGMENTS

We thank all authors for their invaluable contributions to this project. We thank Prof. Bin Chen's group from the University of Electronic Science and Technology of China for their support of this work. We thank Assoc. Prof. Lingnan He from Sun Yat-sen University and Prof. Kaisheng Lai from Jinan University for their professional guidance in psychology. We disclose that the example social media posts illustrated in the Information Domain of Figure 1 were generated by the Nano Banana2 model and do not represent real user content.

REFERENCES

- [1] R. A. Sheikhi, R. Javanbakhtian, and M. Heidari, "Looting and antisocial behavior after disasters: a systematic review," *BMC Public Health*, vol. 25, no. 1, p. 309, 2025.
- [2] D. R. Garfin, R. C. Silver, F. J. Ugalde, H. Linn, and M. Inostroza, "Exposure to rapid succession disasters: a study of residents at the epicenter of the Chilean bio bio earthquake," *Journal of abnormal psychology*, vol. 123, no. 3, p. 545, 2014.

- [3] X. Wu, L. Lu, M. Dotoli, G. Fortino, and M. Chen, "A novel agent-based approach for dynamic emotion modeling in social networks," *IEEE Transactions on Cybernetics*, 2025.
- [4] C. Adam and B. Gaudou, "Bdi agents in social simulations: a survey," *The Knowledge Engineering Review*, vol. 31, no. 3, pp. 207–238, 2016.
- [5] T. Ren, Y. Fan, Z. He, R. Huang, J. Dai, C. Huang, Y. Jing, K. Zhang, Y. Yang, and X. S. Wang, "Purple: Making a large language model a better sql writer," in *2024 IEEE 40th International Conference on Data Engineering (ICDE)*, pp. 15–28, IEEE, 2024.
- [6] Y. Cao, Z. Gao, Z. Li, X. Xie, S. K. Zhou, and J. Xu, "Lego-graphrag: Modularizing graph-based retrieval-augmented generation for design space exploration," *Proceedings of the VLDB Endowment*, vol. 18, p. 3269–3283, June 2025.
- [7] Y. Zhou, Y. Su, Y. Sun, S. Wang, T. Wang, R. He, Y. Zhang, S. Liang, X. Liu, Y. Ma, and Y. Fang, "In-depth analysis of graph-based rag in a unified framework," *Proc. VLDB Endow.*, vol. 18, p. 5623–5637, Sept. 2025.
- [8] W. Wu, H. Wang, B. Li, P. Huang, X. Zhao, and L. Liang, "Multirag: a knowledge-guided framework for mitigating hallucination in multi-source retrieval augmented generation," in *2025 IEEE 41st International Conference on Data Engineering (ICDE)*, pp. 3070–3083, IEEE, 2025.
- [9] D. C. Ong, J. Zaki, and N. D. Goodman, "Computational models of emotion inference in theory of mind: A review and roadmap," *Topics in cognitive science*, vol. 11, no. 2, pp. 338–357, 2019.
- [10] D. Xue, J. Cui, S. Qian, C. Hu, and C. Xu, "Some: A realistic benchmark for llm-based social media agents," in *Proceedings of the AAAI Conference on Artificial Intelligence*, vol. 40, pp. 1391–1399, 2026.
- [11] X. Wang, L. Zhang, Y. Lin, Y. Zhao, and X. Hu, "Computational models and optimal control strategies for emotion contagion in the human population in emergencies," *Knowledge-Based Systems*, vol. 109, pp. 35–47, 2016.
- [12] T. WANG, T. LIU, and C. LI, "Modeling the spread of negative emotions in social networks during sudden public crisis events: Dual mechanisms of social reinforcement and individual regulation," *Journal of Tsinghua University (Science and Technology)*, vol. 65, no. 6, pp. 1040–1049, 2025.
- [13] M. Chu, W. Song, Z. Zhao, T. Chen, and Y.-c. Chiang, "Emotional contagion on social media and the simulation of intervention strategies after a disaster event: A modeling study," *Humanities and Social Sciences Communications*, vol. 11, no. 1, 2024.
- [14] R. Zhao, B. Wei, C. Han, P. Jia, W. Zhu, C. Li, and Y. Ma, "Improved crowd dynamics analysis considering physical contact force and panic emotional propagation," *IEEE Transactions on Intelligent Transportation Systems*, vol. 26, no. 2, pp. 1840–1851, 2024.
- [15] J. S. Park, J. O'Brien, C. J. Cai, M. R. Morris, P. Liang, and M. S. Bernstein, "Generative agents: Interactive simulacra of human behavior," in *Proceedings of the 36th annual acm symposium on user interface software and technology*, pp. 1–22, 2023.
- [16] J. Piao, Y. Yan, J. Zhang, N. Li, J. Yan, X. Lan, Z. Lu, Z. Zheng, J. Y. Wang, D. Zhou, *et al.*, "Agentsociety: Large-scale simulation of llm-driven generative agents advances understanding of human behaviors and society," 2025.
- [17] Y. Hu, G. Sherpa, L. Zhang, W. Li, Q. Bai, Y. Wang, and X. Wang, "An llm-enhanced agent-based simulation tool for information propagation," in *IJCAI*, pp. 8679–8682, 2024.
- [18] L. Wang, H. Gao, X. Bo, X. Chen, and J.-R. Wen, "Yulan-onesim: Towards the next generation of social simulator with large language models," in *Workshop on Scaling Environments for Agents*, 2025.
- [19] Z. Shen, Y. Pang, Y. Rao, and J. Yu, "Coe: A clue of emotion framework for emotion recognition in conversations," in *Proceedings of the 63rd Annual Meeting of the Association for Computational Linguistics (Volume 1: Long Papers)*, pp. 23548–23563, 2025.
- [20] A. Ortony, G. L. Clore, and A. Collins, *The cognitive structure of emotions*. Cambridge university press, 2022.
- [21] Y. Wang, Z. Liu, T. Liu, A. V. Samsonovich, and V. V. Klimov, "On the logic of agent's emotions," *Cognitive Systems Research*, vol. 88, p. 101281, 2024.
- [22] L. Zhong, S. Zhu, Z. Yuan, J. Cui, X. Zhao, L. Wang, H. Chen, and Q. Liao, "Modeling multi-dimensional cognitive states in large language models under cognitive crowding," *arXiv preprint arXiv:2604.17174*, 2026.
- [23] A. S. Rao, M. P. Georgeff, *et al.*, "Bdi agents: from theory to practice," in *Icmas*, vol. 95, pp. 312–319, 1995.
- [24] L. De Silva, F. Meneguzzi, and B. Logan, "Bdi agent architectures: A survey," in *29th International Joint Conference on Artificial Intelligence, IJCAI 2020*, International Joint Conferences on Artificial Intelligence, 2020.
- [25] E. Hatfield, J. T. Cacioppo, and R. L. Rapson, "Emotional contagion," *Current directions in psychological science*, vol. 2, no. 3, pp. 96–100, 1993.
- [26] J. McLennan, M. D. Marques, and D. Every, "Conceptualising and measuring psychological preparedness for disaster: The psychological preparedness for disaster threat scale," *Natural Hazards*, vol. 101, no. 1, pp. 297–307, 2020.
- [27] E. Bulloch, "Psychical distance" as a factor in art and an aesthetic principle," *Journal of Psychology*, vol. 5, no. 2, pp. 87–118, 1912.
- [28] Y. Trope and N. Liberman, "Construal-level theory of psychological distance," *Psychological review*, vol. 117, no. 2, p. 440, 2010.
- [29] Y. Trope, N. Liberman, and C. Wakslak, "Construal levels and psychological distance: Effects on representation, prediction, evaluation, and behavior," *Journal of consumer psychology*, vol. 17, no. 2, pp. 83–95, 2007.
- [30] B. P. Smyth and A. Roche, "Recipient syringe sharing and its relationship to social proximity, perception of risk and preparedness to share," *Addictive Behaviors*, vol. 32, no. 9, pp. 1943–1948, 2007.
- [31] A. Gattig and L. Hendrickx, "Judgmental discounting and environmental risk perception: Dimensional similarities, domain differences, and implications for sustainability," *Journal of Social Issues*, vol. 63, no. 1, pp. 21–39, 2007.
- [32] S. She, M. Chao-Qun, L. Qiang, and C. Xie, "Psychological distance model for environmental risk communication," *Syst. Eng.*, vol. 9, 2012.
- [33] N. Liberman, Y. Trope, E. Stephan, *et al.*, "Psychological distance," *Social psychology: Handbook of basic principles*, vol. 2, no. 2, pp. 353–383, 2007.
- [34] R. S. Lazarus, "Psychological stress and the coping process," *The American Journal of Psychology*, vol. 83, no. 4, 1966.
- [35] A. W. Kruglanski and D. M. Webster, "Motivated closing of the mind: 'seizing' and 'freezing,'" *Psychological review*, vol. 103, no. 2, p. 263, 1996.
- [36] M. Liu, Z. Zhu, C. Ai, C. Gao, X. Li, L. He, K. Lai, Y. Chen, X. Lu, Y. Li, *et al.*, "Psychoagent: Psychology-driven llm agents for explainable panic prediction on social media during sudden disaster events," in *Proceedings of the 2025 Conference on Empirical Methods in Natural Language Processing*, pp. 17127–17145, 2025.
- [37] Y. Kryvasheyev, H. Chen, E. Moro, P. Van Hentenryck, and M. Cebrían, "Performance of social network sensors during hurricane sandy," *PLoS one*, vol. 10, no. 2, p. e0117288, 2015.
- [38] F. M. Bass, "A new product growth for model consumer durables," *Management science*, vol. 15, no. 5, pp. 215–227, 1969.
- [39] R. Muslim, R. A. Nqz, and M. A. Khalif, "Mass media and its impact on opinion dynamics of the nonlinear q-voter model," *Physica A: Statistical Mechanics and its Applications*, vol. 633, p. 129358, 2024.
- [40] F. Yin, N. Jiang, A. Crooks, and L. Laurian, "Agent-based modeling of covid-19 vaccine uptake in new york state: Information diffusion in hybrid spaces," in *Proceedings of the 7th ACM SIGSPATIAL International Workshop on GeoSpatial Simulation*, pp. 11–20, 2024.
- [41] A. N. N. Rende, T. Yilmaz, and O. Ulusoy, "Crowd: A social network simulation framework," *IEEE Transactions on Computational Social Systems*, 2025.
- [42] P. Wu, S. Qiang, and Q. Gao, "Modelling internet users' negative emotion based on soar model," *Chin J Manag Sci*, vol. 26, no. 3, pp. 126–138, 2018.
- [43] D. Naskar, E. Onaindia, M. Rebollo, and S. R. Singh, "Predicting emotion dynamics sequence on twitter via deep learning approach," in *Proceedings of the 18th International Conference on Advances in Mobile Computing & Multimedia*, pp. 20–24, 2020.
- [44] D. Wang, W. Zhou, and S. Hu, "Information diffusion prediction with graph neural ordinary differential equation network," in *Proceedings of the 32nd ACM International Conference on Multimedia*, pp. 9699–9708, 2024.
- [45] Z. Huang, J. Zhao, and Q. Jin, "Ecr-chain: Advancing generative language models to better emotion-cause reasoners through reasoning chains," *arXiv preprint arXiv:2405.10860*, 2024.
- [46] J. E. Zhang, J. Broekens, and J. P. Jokinens, "Modeling cognitive-affective processes with appraisal and reinforcement learning," *IEEE Transactions on Affective Computing*, vol. 16, no. 2, pp. 771–782, 2024.